Accepted Manuscript

Title: Catalytic oxidation of *n*-butanol over platinum supported mesoporous silica CMI-1

Author: Smaïn Sabour Catherine Especel Céline Fontaine Mourad Bidaoui Lakhdar Benatallah Naima Saib-Bouchenafa Jacques Barbier Jr Ourida Mohammedi

PII: S1381-1169(16)30128-5
DOI: http://dx.doi.org/doi:10.1016/j.molcata.2016.04.006
Reference: MOLCAA 9850

To appear in: *Journal of Molecular Catalysis A: Chemical*

Received date: 4-3-2016
Revised date: 22-3-2016
Accepted date: 9-4-2016

Please cite this article as: Smaïn Sabour, Catherine Especel, Céline Fontaine, Mourad Bidaoui, Lakhdar Benatallah, Naima Saib-Bouchenafa, Jacques Barbier, Ourida Mohammedi, Catalytic oxidation of n-butanol over platinum supported mesoporous silica CMI-1, Journal of Molecular Catalysis A: Chemical http://dx.doi.org/10.1016/j.molcata.2016.04.006

This is a PDF file of an unedited manuscript that has been accepted for publication. As a service to our customers we are providing this early version of the manuscript. The manuscript will undergo copyediting, typesetting, and review of the resulting proof before it is published in its final form. Please note that during the production process errors may be discovered which could affect the content, and all legal disclaimers that apply to the journal pertain.

ACCEPTED MANUSCRIPT

Catalytic oxidation of *n*-butanol over platinum supported mesoporous silica CMI-1

Smaïn Sabour[1], Catherine Especel[2*], Céline Fontaine[2], Mourad Bidaoui[3], Lakhdar Benatallah[1], Naima Saib-Bouchenafa[1], Jacques Barbier Jr[2], Ourida Mohammedi[1]

[1] *Université Blida 1, Laboratoire de Chimie Physique Moléculaire et Macromoléculaire (LCPMM), BP270, route Somaa, Blida, Algeria*

[2] *Université de Poitiers, CNRS UMR 7285 IC2MP, Institut de Chimie des Milieux et des Matériaux de Poitiers, 4 rue Michel Brunet, TSA 51106, 86073 Poitiers Cedex 9, France*

[3] *Centre Universitaire de Tissemsilt, Institut des Sciences et Technologies, Abdelhak Benhamouda BP182, Tissemsilt 38000, Algeria*

* Corresponding author: Catherine Especel catherine.especel@univ-poitiers.fr

Tel.: +33 5 49 45 39 94

ACCEPTED MANUSCRIPT

Graphical abstract

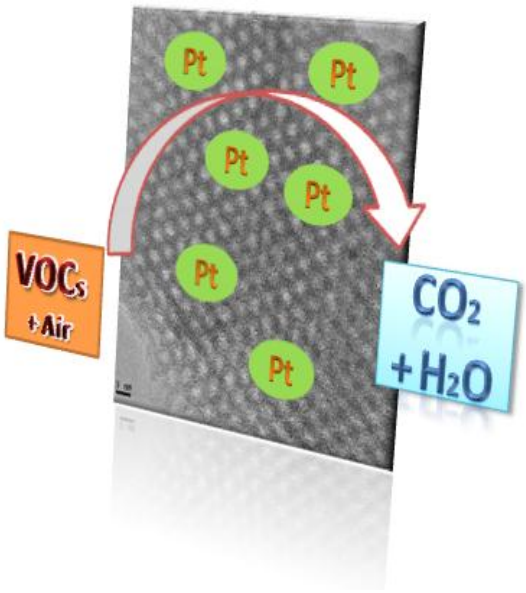

ACCEPTED MANUSCRIPT

Highlights

- Total oxidation of *n*-butanol was studied on mesoporous silica-supported catalysts.
- The conversion varied as follows according to the metallic phase: Pt > Pd > Rh > Au.
- For the Pt/CMI-1 synthesis, the use of a Cl-based salt led to a less active sample.
- The catalytic behavior of Pt catalysts supported on various supports was compared.
- The Pt-based systems activity was governed by the support specific surface area.

ACCEPTED MANUSCRIPT

Abstract

n-butanol oxidation was studied using noble metals (Pt, Pd, Rh and Au) supported on a highly structured mesoporous material: CMI-1. The catalysts were characterized by several physico-chemical techniques, *i.e.* N_2 sorption, ICP, H_2 chemisorption, XRD and TEM. The Pt based catalyst was the most active material, followed by Pd/CMI-1, Rh/CMI-1 and Au/CMI-1. Difference in size of the particles was proposed as origin of these results, this parameter being well-known to strongly influence the catalytic activity. The comparison of two Pt/CMI-1 catalysts prepared from various precursor salts (with and without chlorine) showed that *n*-butanol oxidation was sensitive to the nature of the metallic salt. Finally the modifications induced by the nature of the support were studied by comparing Pt/Al_2O_3 and Pt/TiO_2 systems. Pt dispersion and specific surface area of the support seemed to be important parameters influencing the activity of the materials. In the studied conditions, Pt/CMI-1 was still the most active catalyst.

Keywords

Mesoporous silica, CMI, Platinum, *n*-butanol, Oxidation.

ACCEPTED MANUSCRIPT

1. Introduction

Volatile organic compounds (VOC) contribute significantly to the air pollution by their toxic nature and/or by the formation of photochemical smog [1,2]. As a result, research on VOC elimination has attracted more interest over the last decade, with the development of efficient catalysts in VOC total oxidation including precious metals and transition metals oxides [3,4]. Despite their expensive cost, the noble metal catalysts are preferred due to their high activity, their resistance to deactivation and their possible regeneration [2]. Catalytic performances of supported noble metals depend strongly on the preparation method, the nature of the metallic precursor, the metal particle size, the metal content and the nature of the support [5-7]. In addition, the nature of VOC, the operating conditions used such as oxygen concentration and the global gas flow also have a noticeable influence on catalytic performances [8,9].

Among noble metals cited in the literature, platinum and palladium are the most studied. Santos *et al.* [10] compared a series of noble metals supported on titania for the oxidation of three VOC, and noticed that Au/TiO_2 catalyst was the most active for the conversion of carbon monoxide, while in the case of the ethanol and toluene oxidation the catalytic performances were ordered as follows: $Pt/TiO_2 > Pd/TiO_2 > Rh/TiO_2 > Ir/TiO_2 > Au/TiO_2$. A similar study devoted to the formaldehyde oxidation showed also the catalytic superiority of platinum- and palladium-based systems [11]. By studying the catalytic oxidation of butanol, benzene and ethyl acetate, Papaefthimiou *et al.* [12] concluded that catalysts containing platinum are generally more active than those with palladium.

Concerning the effect of the support nature, Peng *et al.* showed the efficiency of Pt/TiO_2 systems for formaldehyde oxidation compared to Pt-based catalysts involving other supports such as SiO_2 or CeO_2-ZrO_2 mixed oxides [11]. These authors considered that the catalytic properties were not only linked to the nature of the support but also to the metal dispersion. During the oxidation of ethyl acetate on Pt-based catalysts, Papaefthimiou *et al.* [13] have highlighted the benefit influence of the

ACCEPTED MANUSCRIPT

acidic properties of the support by comparing TiO_2 and W-doped TiO_2 displaying a higher density of acid sites.

For some authors, the effect of the support hydrophobicity plays a decisive role in VOC oxidation. Chuang *et al.* [14], by comparing the activities of Pt catalysts supported on hydrophobic and hydrophilic materials, noticed that the oxidation can be achieved at low temperature on hydrophobic supports. Similar results were obtained by Wu and Wang for the toluene oxidation on Pt catalysts deposited on hydrophobic supports [15].

Some authors have recently reported the interest in using mesoporous silica materials as catalyst supports for VOC oxidation [16-19], due to their high specific surface areas and pore volumes [20] and their great thermal and mechanical stabilities [21]. In this context, this work is mainly dedicated to the use of a specific silicic support highly structured (CMI-1, [22]) for *n*-butanol oxidation.

2. Experimental part

2.1. Catalysts preparation

The CMI-1 silica was synthesized according to the protocol described by Leonard *et al*. [23], using decaoxyethylene cetyl ether [C16(EO)10, Brij 56®], tetramethoxysilane (TMOS, 98%) and sulfuric acid (H_2SO_4, 98%).The synthesis of mesoporous alumina was performed by dissolution of 7.5 g of Pluronic® (P123, $PEO_{20}PPO_{70}PEO_{20}$) in 150 mL of ethanol with 11 mL of HNO_3 (70%), under stirring at room temperature. After the complete dissolution of P123, 30.75 g of aluminum isopropoxide was added and the mixture was kept under stirring for 5 h, and further dried in an oven at 60°C. The gel obtained is calcined under air at 600°C (1°C.min^{-1}) during 6 h. TiO_2 support (99.9%) was provided by Alfa Aesar.

Pt/CMI-1, Pd/CMI-1, Rh/CMI-1 and Au/CMI-1 catalysts with a 0.5 wt% expected metallic content were prepared from H_2PtCl_6 (Aldrich), $PdCl_2$ (Aldrich), $Rh(NO_3)_2$ (Aldrich) and $HAuCl_4$ (Fisher) precursor solutions, respectively. The precursor solution was dissolved in 50 mL of ultrapure water,

ACCEPTED MANUSCRIPT

the pH was further adjusted to 2 (or between 8 and 9 in the case of Au-based catalyst) and then the CMI-1 support was added. The solution was kept under stirring at room temperature for 2 h, and the excess of solvent was removed by evaporation in a sand bath overnight. The samples were calcined under air at 300°C (1°C.min^{-1}) for 3 h.

Pt(acac)/CMI-1, Pt(acac)/Al_2O_3 and Pt(acac)/TiO_2 catalysts were also prepared using platinum acetylacetonate precursor dissolved in 25 mL of toluene (Aldrich, 99.8%). After elimination of the solvent by rotary evaporator, the solid was dried at 120°C overnight and then calcined under air at 400°C (1°C.min^{-1}) during 3 h to ensure the total elimination of toluene.

2.2. Catalysts characterization

The metal content of the catalysts was determined by ICP-OES (Inductively Coupled Plasma Optical Emission Spectrometer) on a Perkin-Elmer Optima 2000 device.

Physical properties of the materials (specific surface area, average pore size distribution and pore volume) were obtained from N_2-sorption isotherms collected at -196°C on a Micromeritics Tristar 3000 apparatus. Samples were previously degassed for one night at 250°C until a residual pressure below 0.15 mbar. The specific surface area was determined from the linear part of the BET plot, the mesopore size distribution by the NLDFT (non local density functional theory) method and using the Autosorb-1 1.52 software. The kernel selected was N_2 on silica assuming cylindrical pore geometry and the equilibrium based on the desorption branch. Pore volume was determined on the isotherms at $P/P_0 = 0.97$.

The characterizations by powder X-ray diffraction (XRD) were performed on a diffractometer PANalytical Empyrean equipped with a copper anode as X-ray source (CuKα radiation, $\lambda = 1.54186$ Å). The patterns were recorded for 2θ comprised between 0.75° and 5° with a step of 0.01° (step time of 10 s) and between 10° and 70° with a step of 0.05° (step time of 2 s). Phase identification was made by comparison with JCPDS database. The lattice parameter (a_0) of the structure

ACCEPTED MANUSCRIPT

corresponding to the sum of the pore internal diameter and the thickness of the silica wall was calculated from the relation $a_0 = (2/\sqrt{3}).d_{100}$, with d_{100} issued from by Bragg formula $2d_{100} \sin\theta = n\lambda$. The size distribution of metal particles in the mesoporous structure was measured by Transmission Electron Microscopy (TEM) on a JEOL 2100 UHR device (LaB_6 source, 200 kV) equipped with a Gatan Ultra scan camera. The samples were embedded in a polymeric resin (spur), cut into small sections (50 nm) with an ultramicrotome equipped with a diamond knife, and then deposited on a Cu grid holey carbon film. Average particle size of each analyzed sample was determined by measuring at least 100 particles, from at least 5 different micrographs.

Hydrogen chemisorption was performed to determine metal dispersion by using a classical pulsed technique. After reduction of the sample under H_2 (1.8 $L.h^{-1}$, 1 h, 300°C), the reactor was flushed by Ar flow (1.8 $L.h^{-1}$) at the same temperature for 2 h before being cooled down to ambient temperature. H_2 pulses (0.25 mL) were injected at regular intervals, and the dispersion values were calculated by assuming an H/surface metal atom stoichiometry equal to 1. From the amount of H_2 consumed, the average particle size was calculated using the equation as described elsewhere [24].

2.3. Catalytic test of n-butanol oxidation

Experiments were performed according to the protocol established by Sedjame *et al.* [25]. The gaseous feed used for the catalytic tests was composed of 1000 ppm of VOC in synthetic air. VOC and water were heated in two thermostated saturators. Nitrogen was bubbled through these saturators and the outflow was mixed with the synthetic air. At the reactor inlet the gas stream was composed of 19.38% of O_2, 77.52% of N_2, 3% of H_2O and 0.1% of VOC. Transfer lines were heated at 110°C to avoid any condensation. The total flow rate was kept constant for all experiments (70 mL min^{-1}). Reactions were carried out in a tubular fixed bed reactor placed in an electrical furnace equipped with a temperature programmer. A thermocouple was inserted in the reactor near the catalyst bed to measure exactly the reaction temperature. A mass of 140 mg of catalyst mixed with 1 g of cordierite

ACCEPTED MANUSCRIPT

were used for the reactions. The space velocity was 60000 h^{-1}. The reaction products were analyzed by a Gas Chromatograph (Varian 490-GC) equipped with a thermal conductivity detector (TCD) and two columns: a Porapak Q (PPQ) to analyze air and carbon dioxide and a CP sil-5CB to analyze hydrocarbons (butanol, butanal, acetic acid...). Experiments were performed between 50 and 350°C and the temperature was increased linearly by 0.5°C min^{-1}. The uncertainty on the results is about ± 1°C.

3. Results and discussion

3.1. Characterization of the M/CMI-1 catalysts

Four 0.5 wt% M/CMI-1 samples (with M = Pt, Pd, Rh or Au) were first prepared using the CMI-1 support previously synthesized. The main physical and structural characteristics of the CMI-1 support and these catalysts (Table 1) showed that the prepared samples belonged to the family of mesoporous solids, with a high specific surface area and a significant thickness of the walls (≥ 20 Å).

Table 1: Specific surface areas, pore volumes, average pore diameters, lattice parameters and dispersions of CMI-1 supported catalysts

	CMI-1	**Pt/CMI-1**	**Pd/CMI-1**	**Rh/CMI-1**	**Au/CMI-1**
Specific surface area ($m^2.g^{-1}$)	846	835	824	835	845
Pore diameter D_P (Å)	26.3	26.1	26.0	26.2	26.3
Pore volume ($cm^3.g^{-1}$)	0.97	0.97	0.97	0.97	0.97
Lattice parameter a_0 (Å)	51.1	51.7	51.7	51.4	51.1
Wall thickness W[a] (Å)	24.8	25.6	25.7	25.2	24.8
Metal content (wt.%)	-	0.4	0.5	0.6	0.5
Average metal particle size[b](Å)	-	14 (13)	15	17	-
Metal dispersion (%)	-	66	-	-	-

[a] $W = a_0 - D_P$

[b] Determined by TEM analysis (between bracket, value calculated from dispersion value)

N_2-sorption isotherm of the CMI-1 material (Fig. 1A) was of type IV according to the IUPAC classification, which is consistent with the formation of organized mesoporous materials [26]. The low angle X-ray powder diffraction pattern of the CMI-1 support (Fig. 2A) exhibited a very intense peak as well as two other undefined peaks, corresponding to reflections on the (100), (110) and (200)

ACCEPTED MANUSCRIPT

planes of a 2D hexagonal structure as observed by Ren *et al.* [20]. At large angles (Fig. 2B), the CMI-1 sample displayed a wide diffraction peak of $2\theta \approx 23°$ attributed to amorphous silica [27]. A honeycomb network with a hexagonal pore arrangement was clearly confirmed for the CMI-1 material by TEM analysis (Fig. 3A).

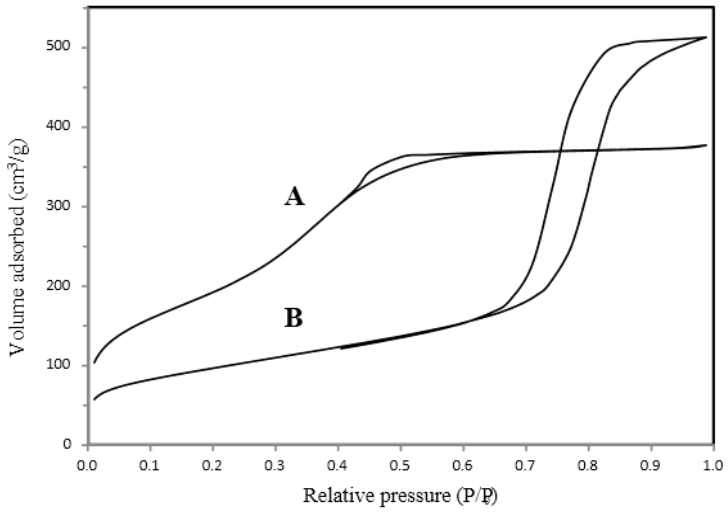

Fig. 1. N_2-sorption isotherms of CMI-1 (A) and Al_2O_3 (B) synthesized supports.

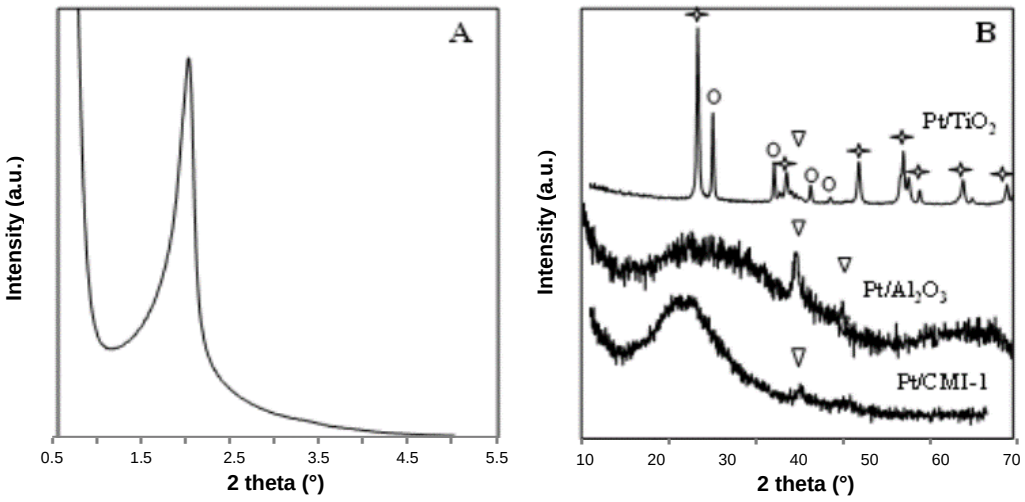

Fig. 2. X-ray diffraction patterns: (A) small angle of the CMI-1 support and (B) wide angle of the Pt-based catalysts (prepared from Pt acetylacetonate precursor salt).
▽ : Pt phase; ✧ anatase phase; ○ rutile phase

ACCEPTED MANUSCRIPT

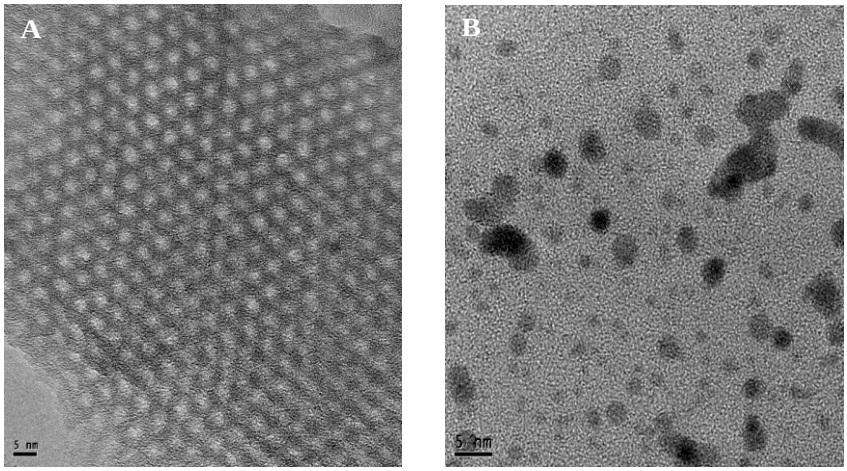

Fig. 3. TEM images of (A) CMI support and (B) 0.5 wt% Pt/CMI-1.

As showed in Table 1, after impregnation of the CMI-1 support by metals (deposited content of 0.5 ± 0.1 wt% according to the experimental values determined by ICP-OES), each catalyst displayed a high specific surface area in the same range of order than that of the lone support (835 ± 10 $m^2.g^{-1}$). Moreover, the pore volume (0.97 $cm^3.g^{-1}$) and pore diameter (D_P = 26.15 ± 0.15 Å), as well as the lattice parameter (a_0 = 51.4 ± 0.3 Å) and wall thickness (W = 25.25 ± 0.45 Å), remained unchanged after the metal impregnation on the CMI-1 support indicating that the deposition of the metal (whatever its nature) did not affect the structure of the mesoporous oxide. On Fig. 3B showing a TEM representative image of the Pt/CMI-1 catalyst, the metallic particles appear well dispersed. The analysis by TEM of the Pd/CMI-1 and Rh/CMI-1 catalysts (images not shown) led to the same observation, whereas no detection of Au particles was possible indicating that the particles of the Au/CMI-1 sample are too small for the microscope resolution. From TEM images, average particle sizes of 14 Å, 15 Å and 17 Å were estimated for the Pt/CMI-1, Pd/CMI-1 and Rh/CMI-1 catalysts, respectively. In the case of the Pt/CMI-1 sample, this average size is in accordance with the one determined from the metal dispersion value (Table 1). In fact, from hydrogen chemisorption experiments, the Pt phase dispersion was estimated to 66% which corresponds to an average particle size of 13 Å [24], *i.e.* very slightly lower than that calculated by TEM. The difference can be explained by the existence of small particles not observed by TEM analysis.

ACCEPTED MANUSCRIPT

3.2. Catalytic transformation of n-butanol on the M/CMI-1 catalysts

3.2.1. Effect of the presence of steam

A preliminary test of *n*-butanol oxidation was performed on the Pd/CMI-1 catalyst in presence and absence of water steam in the gas feed. The plots of *n*-butanol conversion to CO_2 obtained for each experiment (Fig. 4) clearly show that there is no effect of steam on the oxidation reaction with these catalysts. Conversely, a recent study dealing with Pt/Al_2O_3 catalysts showed the inhibiting effect of steam on the oxidative removal of the *n*-butyl alcohol [25]. Consequently, the present result highlights the interest of using support displaying hydrophobic sites for VOC oxidation reactions [28,29]. Indeed, mesoporous silica-based materials such as CMI-1 possess different groups on their surface, including silanols (Si-OH) and siloxanes (Si-O-Si) [30]. Siloxanes are considered to be hydrophobic sites generated by dehydroxylation during heat treatment [28,29], while the silanol groups are considered as weak acid sites [31]. In order to stay as close as possible to the real conditions, water steam has been added to the feed for the experiments performed in the rest of the manuscript.

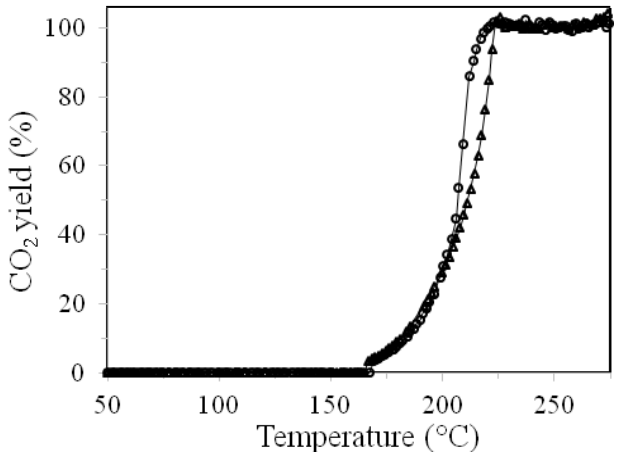

Fig. 4. CO_2 yield during *n*-butanol transformation on Pd/CMI-1: influence of the presence (○) and absence (△) of steam in the gas feed.

3.2.2. Effect of the nature of the metal

ACCEPTED MANUSCRIPT

The behavior of the four M/CMI-1 (M = Pt, Pd, Rh or Au) catalysts was evaluated for the oxidation of *n*-butanol conducted in the presence of steam (Fig. 5). The activities of the materials are compared in term of light-off, *i.e.* the temperature necessary to convert 50% (T_{50}) or 90% (T_{90}) of the reactant: the lower is the T_{50} or T_{90}, the more active is the catalyst. Following this criteria, the activity of the different catalysts for the total conversion to CO_2 was classified as follows: Pt/CMI-1 > Pd/CMI-1 > Rh/CMI-1 > Au/CMI-1. The Au/CMI-1 catalyst led to the lowest conversion of *n*-butanol (T_{50} = 257°C and T_{90} > 300°C for 50% and 90% conversion, respectively). By comparison, the T_{50} temperature observed for the Rh/CMI-1 sample was quite similar (254°C) but the T_{90} was lowered to 287°C. The presence of Pd on the CMI-1 support involved a noticeable improvement of the activity since 50% and 90% of conversions were obtained at 207 and 214°C, respectively. Finally, with the Pt/CMI-1 sample, a new decrease approximately of 23°C was achieved for the T_{50} temperature (T_{50}= 184°C), a lower one being observed for T_{90} (T_{90} = 208°C). As seen previously, these CMI-1 supported catalysts exhibit a mesoporous structure with comparable high specific surface areas and wall thicknesses allowing them to present a thermal stability [32]. The different activities observed here are undeniably linked to the nature of the metal, since the metal particle sizes are not so different for all M/CMI-1 catalysts (Table 1).

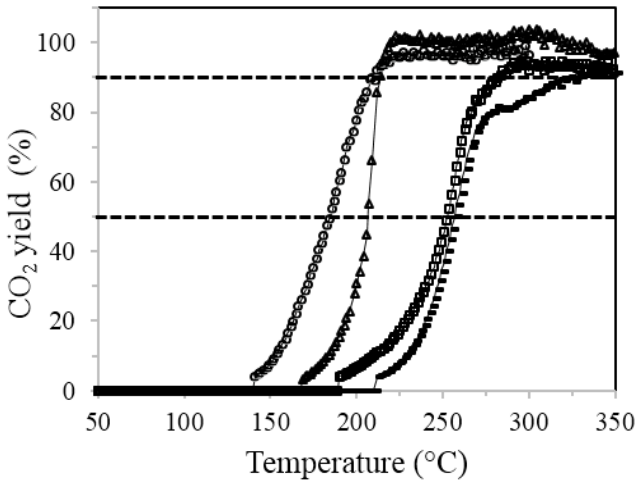

Fig. 5. CO_2 yield during *n*-butanol transformation on M/CMI-1: Pt (○), Pd (△), Rh (□), Au (-).

ACCEPTED MANUSCRIPT

3.2.3. Effect of the nature of the metallic precursor salt

As Pt/CMI-1 was the most active catalyst, we focused on this catalyst to study the influence of the nature of the Pt precursor salt on its behavior during the catalytic oxidation of *n*-butanol. Two 0.5 wt% Pt/CMI-1 catalysts prepared from two precursor salts of platinum were compared (Fig. 6): the previous sample Pt/CMI-1 synthesized from H_2PtCl_6 and a new one Pt(acac)/CMI-1 issued from platinum acetylacetonate impregnation (the characteristics of this sample are given in Table 2).

Table 2: Characteristics of the Pt(acac) catalysts supported on CMI-1, Al_2O_3 and TiO_2

	Pt(acac)/CMI-1	**Pt(acac)/Al_2O_3**	**Pt(acac)/TiO_2**
Specific surface area (m^2/g)	833	177	45
Pore diameter D_P (Å)	26	12	23
Pt content (wt.%)	0.5	0.5	0.5
Pt dispersion (%)	59	69	80
Average metal particle size[a] (Å)	14	12	11

[a]Value calculated from dispersion value

The comparison of the CO_2 formation curves clearly showed that the Pt(acac)/CMI-1 catalyst was the most active: by replacing the H_2PtCl_6 precursor salt by the Pt acetylacetonate free-chlorinated one, the T_{50} temperature decreased from 184°C to 130°C and the T_{90} value from 208°C to 191°C. Since the textural properties were quite comparable for both samples (Tables 1 and 2), as well as the average metal particles (13-14Å), the residual chlorides on the Pt/CMI-1 catalyst were supposed to have a detrimental effect on the *n*-butanol conversion. It is well known that the preparation process and the nature of the metal precursors used, such as chlorinated salts, can affect the properties of the catalysts because the thermal treatment by calcination under air does not allow the complete removal of the chloride ions [33]. Even if catalysts prepared from chloride salts often present a higher metal dispersion, their catalytic activity can be lower than previously observed for example for the complete oxidation of propene and toluene on Pt/γ-Al_2O_3 catalysts prepared by impregnation from either $Pt(NH_3)_4(OH)_2$ or H_2PtCl_6 solution [5,7,34]. The detrimental effect of chloride was explained by a partial blockage of the active metal sites involving a decrease of their ability to activate the

ACCEPTED MANUSCRIPT

reagent molecules [34,35]. In addition, the formation of less active $M_xO_yCl_z$ oxochlorinated species was also mentioned [5,36,37].

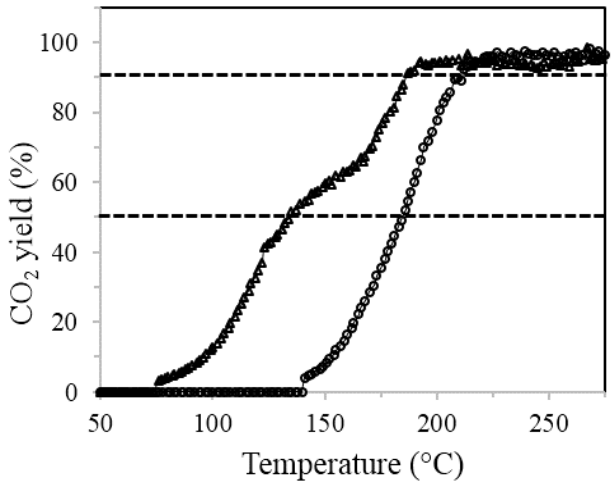

Fig. 6. CO_2 yield during *n*-butanol transformation on Pt/CMI-1(○) and Pt(acac)/CMI-1 (△).

3.2.4. Effect of the nature of the support

From the Pt acetylacetonate precursor salt, two other catalysts Pt(acac)/Al_2O_3 and Pt(acac)/TiO_2 were prepared by varying the nature of the support and compared with the Pt(acac)/CMI-1 sample (Table 2). The Pt(acac)/Al_2O_3 sample prepared from the synthesized alumina support displayed a much lower specific surface area than the one of Pt(acac)/CMI-1 (177 compared to 833 $m^2.g^{-1}$), this surface reached 45 $m^2.g^{-1}$ for the Pt(acac)/TiO_2 catalyst prepared form the commercial titania. After the deposit of 0.5 wt.% Pt, the metal dispersion was measured by XRD and the average particle size was evaluated to 14, 12 and 11 Å on the CMI-1, Al_2O_3 and TiO_2 supports, respectively. The presence of diffraction peaks located at 2θ = 40°, 46° and 68° and attributed to platinum phase was detected on these three catalysts, as well as a mixture of anatase and rutile phases in the case of the sample supported on titania (Fig. 2B).

Fig. 7 compares the CO_2 yield obtained as function of the temperature during the conversion of *n*-butanol on the three Pt(acac) supported catalysts. The T_{90} temperatures were quite comparable for

ACCEPTED MANUSCRIPT

the three catalysts, but the T_{50} temperatures differed since 130°C, 158°C and 167°C were obtained with CMI-1, Al_2O_3 and TiO_2 supports, respectively.

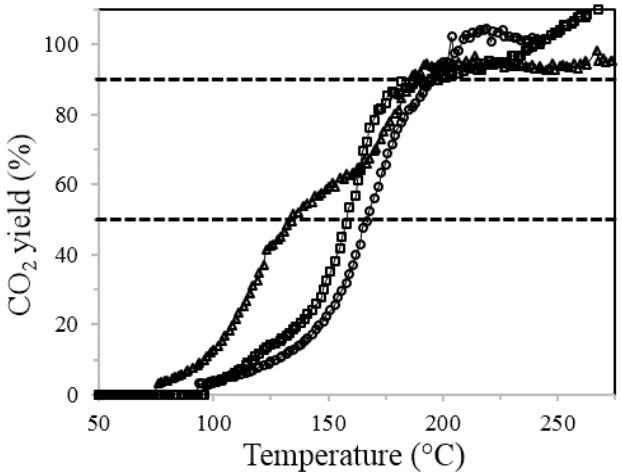

Fig. 7. CO_2 yield during *n*-butanol transformation on Pt(acac) catalysts supported on: CMI-1 (△), Al_2O_3 (□), TiO_2 (○).

The three studied catalysts were prepared by impregnation of the same chlorine-free precursor salt, consequently no residual chlorine species can affect the catalytic behavior. The metallic phase was not dispersed similarly on the various supports, but the Pt(acac)/CMI-1 catalyst with the highest average particle size was finally the most active sample. Several authors related that the dispersion of the active phase is an important factor on the catalytic performances, the metal particle size decrease involving generally a positive effect on the catalytic activity [38-40]. Consequently, the results of Fig. 7 indicate that the parameter explaining the different activities of the three studied catalysts was first the nature of the support. The catalyst supported on CMI-1 presents a large specific surface area which can provide an important contact with *n*-butanol.

4. Conclusions

The following conclusions can be drawn from this study devoted to the catalytic oxidation of *n*-butanol on metallic supported catalysts:

ACCEPTED MANUSCRIPT

- the use of mesoporous CMI-1 support with hydrophobic sites seemed to limit the inhibitory effect of water during VOC oxidation,

- among the studied metals (Pt, Pd, Rh and Au), the Pt-based catalyst was the most active for the catalytic oxidation of *n*-butanol,

- the use of a chlorinated precursor for the preparation of Pt/CMI-1 catalysts induced an inhibiting effect on their activity for *n*-butanol conversion,

- the catalytic activity of supported Pt-based catalysts for *n*-butanol conversion was governed by the specific surface area of the support.

References

[1] H.L. Tidahy, S. Siffert, F. Wyrwalski, J.-F. Lamonier, A. Aboukais, Catal. Today 119 (2007) 317-320.

[2] R.M. Heck, R.J. Farrauto, Catalytic Pollution Control, 2nd ed., Wiley-Interscience, New York (2002).

[3] W.B. Li, J.X. Wang, H. Gong, Catal. Today 148 (2009) 81-87.

[4] C. He, J. Li, X. Zhang, L. Yin, J. Chen, S. Gao, Chem. Eng. J. 180 (2012) 46-56.

[5] M. Paulis, H. Peyrard, M. Montes, J. Catal. 199 (2001) 30-40.

[6] N. Radic, B. Grbic, A. Terlecki-Baricevic, Appl. Catal. B: Environ. 50 (2004) 153-159.

[7] S. Benard, M. Ousmane, L. Retailleau, A. Boreave, P. Vernoux, A. Giroir-Fendler, Can. J. Civil. Eng. 36 (2009) 1935-1945.

[8] V. Perez, S. Miachon, J.-A. Dalmon, R. Bredesen, G. Pettersen, H. Raeder, C. Simon, Sep. Purif. Technol. 25 (2001) 33-38.

[9] S. Benard, A. Giroir-Fendler, P. Vernoux, N. Guilhaume,, K. Fiaty, Catal. Today 156 (2010) 301-305.

ACCEPTED MANUSCRIPT

[10] V.P. Santos, S.A.C. Carabineiro, P.B. Tavares, M.F.R. Pereira, J.J.M. Orfao, J.L. Figueiredo App.Catal. B: Environ. 99 (2010) 198-205.

[11] J.Peng, S. Wang, App. Catal. B: Environ. 73 (2007) 282-291.

[12] P. Papaefthimiou, T. Ioannides, X.E. Verykios, Appl. Catal. B: Environ. 13 (1997) 175-184.

[13] P. Papaefthimiou, T. Ioannides, X.E. Verykios, Catal. Today 54 (1999) 81-92.

[14] K.T. Chuang, B. Zhou, S. Tong, Ind. Eng. Chem. Res. 33 (1994) 1680-1686.

[15] J. Chi-Sheng Wu, T.Y. Chang, Catal. Today 44 (1998) 111-118.

[16] K.H. Chuang, Z.S. Liu, Y.H. Chang, C.Y. Lu, M.Y. Wey, Reac. Kinet. Mech. Catal. 99 (2010) 409-420.

[17] A. De Stefanis, S. Kaciulis, L. Pandolfi, Micro. and Meso. Mater. 99 (2007) 140-148.

[18] C. He, F. Zhang, L. Yue, X Shang, Z. Hao, Appl. Catal. B: Environ. 111-112 (2012) 46-57.

[19] L. Usón, M.G. Colmenares, J.L. Hueso, V. Sebastián, F. Balas, M. Arruebo, J. Santamaría, Catal. Today 227 (2014) 179-186.

[20] T.Z. Ren, Z.Y. Yuan, B.L. Su, Colloids and Surfaces A: Physicochem. Eng. Aspects 300 (2007) 79-87.

[21] K. Cassiers, T. Linssen, M. Mathieu, M. Benjelloun, K. Schrijnemakers, P. Van DerVoort, P. Cool, E.F. Vansant, Chem. Mater. 14 (2002) 2317-2324.

[22] C. Bouvy, W. Marine, R. Sporken, B.L. Su, Chem. Phys. Letters 420 (2006) 225-229.

[23] A. Leonard, J.L. Blin, P.A. Jacobs, P. Grange, B.L. Su, Micro. and Meso. Materials 63 (2003) 59-73.

[24] M. Bidaoui, C. Especel, S. Sabour, L. Benatallah, N. Saib-Bouchenafa, S. Royer, O. Mohammedi J. Mol. Catal. A 339 (2015) 97-105.

[25] H.J Sedjame, G. Lafaye, J. Barbier Jr, Appl. Catal. B: Environ. 132-133 (2013) 132-141.

[26] D. Zhao, J. Sun, Q. Li, G.D. Stucky, Chem. Mater 12 (2000) 275-279.

ACCEPTED MANUSCRIPT

[27] C. He, P. Li, H.L. Wang, J. Cheng, X.Y. Zhang, Y.F. Wang, Z.P. Hao, J. Hazard. Mater 181 (2010) 996-1003.

[28] M.H. Lim, A. Stein, Chem. Mater. 11 (1999) 3285-3295.

[29] L. Mercier, T.J. Pinnavaia, Env. Sci. and Techno. 32 (1998) 2749-2754.

[30] P.K. Jal, S. Patel, B.K. Mishra, Talanta 62 (2004) 1005-1028.

[31] C. Despas, A. Walcarius, J.Bessiere, Talanta 45 (1997) 357-369.

[32] A. Léonard, J.L. Blin, B.L. Su, Colloids and Surfaces A: Physicochem. Eng. Aspects 241 (2004) 87-93.

[33] D. Roth, P. Gélin, M. Primet, E. Tena, Appl. Catal. A 203 (2000) 37-45.

[34] D.I. Kondarides, X.E. Verykios, J. Catal. 174 (1998) 52-64.

[35] G. Pecchi, P. Reyes, R. Gomez, T. Lopez, J.L. Fierro, Appl. Catal. B 17 (1998) L7-L13.

[36] N.W. Cant, D.E. Angove, J.M. Patterson, Catal. Today 44 (1998) 93-99.

[37] S. Scire, S. Minico, C. Crisafulli, Appl. Catal. B: Environ. 45 (2003) 117-125.

[38] C.M. Lu, Y.M. Lin, I. Wang, Appl. Catal. A: Gen. 198 (2000) 223-234.

[39] J.S. Albero, A.S. Escribano, F.R. Reinoso, J.A. Anderson, J. Catal. 223 (2004)179-190.

[40] S. Bernal, J.J. Calvino, M.A. Cauqui, J.M. Gatica, C.L. Cartes, J.A. Perez Omil, J.M. Pintado, Catal. Today 77 (2003) 385-406.